Folded acoustic and confined optical phonons in a $(Si_{15}Ge_4)_{50}$ atomic-layer superlattice

R. W. G. Syme,* D. J. Lockwood, and J.-M. Baribeau
Institute for Microstructural Sciences, National Research Council Canada, Ottawa, Ontario, Canada K1A 0R6
(Received 7 May 1998)

A Raman-scattering intensity analysis of folded acoustic modes in a high-quality $(Si_{15}Ge_4)_{50}$ superlattice has allowed a detailed comparison with various theoretical models. The modulus of the Ge/Si photoelastic coefficient ratio is found to be ~1 at 457.9 nm, but a satisfactory simultaneous fit to all the intensity information could not be obtained with any of the models. The role of an interface translational displacement contribution to the scattering cross section is shown to be significant. Odd and, for the first time, even index confined optic modes are observed for the Si layers in the polarized Raman spectrum. Lower-frequency quasiconfined optic modes exhibit dispersion that is consistent with previous model calculations. [S0163-1829(99)05203-0]

I. INTRODUCTION

Raman-scattering spectroscopy is well established as a valuable and versatile technique in the study of semiconductor superlattices, both for characterizing the superlattice structure and for probing the physical properties of such systems. There has been much work[1,2] relating to III-V superlattices, such as GaAs/AlAs, in which various vibrational features have been identified with propagating, confined or interface modes in these heterostructures. In the case of group-IV (Si/Ge or $Si/Si_{1-x}Ge_x$) superlattices there have been several studies of folded acoustic modes,[3–10] while detailed analyses of optic modes[11–15] have identified quasiconfined Ge-Ge and confined Si-Si modes, around 300 and 500 cm^{-1}, respectively, together with a ''Si-Ge'' feature near 400 cm^{-1} whose position and intensity is particularly sensitive to the interface sharpness. Model calculations[14–19] have elucidated the role of strain and interface quality in determination of the Si/Ge superlattice vibrational spectrum. Confined optic modes can be observed within the Si layers of the superlattices,[12–15] but generally not within the Ge or alloy layers, depending on the Si layer thickness. As a result of the experimental conditions, previous analyses of the Raman scattering from confined modes in group-IV superlattices was restricted to study of odd index modes.[13,15]

As an adjunct to these studies, application of the photoelastic model[20] to light scattering from folded acoustic phonons has been applied to the evaluation of the ratio of $Si_{1-x}Ge_x$ to Si photoelastic coefficients from the spectra of both periodic[21,22] and quasiperiodic[23] superlattices. In the prior studies of $Si/Si_{1-x}Ge_x$ superlattices a wide range of photoelastic constant ratios was obtained[21,22] for $x \cong 0.5$ and values for $x > 0.5$ in the visible-wavelength region are unknown. To define better the trend with increasing x and for further tests of theory[24] it is important to obtain experimental information near $x = 1$.

With continuing modification of growth methods[25,26] it is now possible to produce much better material in Si/Ge atomic-layer superlattices than that used for earlier Raman studies. The availability of such a sample has enabled a detailed analysis of folded acoustic modes in a $(Si_mGe_n)_p$ atomic layer superlattice (where m and n are the numbers of Si and Ge monolayers in each period and p is the number of periods), including the first consideration of information about the relevant photoelastic coefficients of Ge and Si obtainable from the relative intensities of these modes. Although estimates of the Ge/Si photoelastic constant ratio can be obtained from our data, an analysis of *all* $Si/Si_{1-x}Ge_x$ superlattice results obtained to date indicates there are still experimental and theoretical difficulties to be overcome before a fully comprehensive understanding can be reached. Notably, it is clear from this analysis that the interface translational-displacement contribution to the scattering mechanism must be considered. In addition, the observation of a polarization dependence in the Raman spectrum has revealed Si layer confined modes of both even and odd index, analogous to those seen previously only for III-V superlattices.[1] These features are interpreted within a slab-mode model.

II. EXPERIMENT

The $(Si_{15}Ge_4)_{50}$ superlattice studied here was grown on a (001) Si wafer held at 320 ± 50 °C in a VG Semicon V80 molecular-beam-epitaxy system. Further details of the growth methodology and growth parameters for this sample are described elsewhere.[25,26] X-ray diffraction using Cu K_α radiation on a Philips MRD instrument determined the superlattice periodicity of the sample to be 2.58 nm with an average Si-layer thickness of 2.10 ± 0.05 nm and Ge-layer thickness of 0.48 ± 0.05 nm. X-ray specular reflectivity and diffuse-scattering measurements were also carried out on this sample using a Philips PW1820 goniometer. These measurements, described in detail in Ref. 27, confirmed that the sample (referred to as Si1584 in Ref. 27) had a well-defined periodicity and showed that the interfaces were also very sharp (interface width less than 0.5 nm). The interface roughness exhibited some cross correlation (i.e., replication from interface to interface) and was characterized by an undulation in the plane of growth of wavelength ~0.5 mm, predominantly oriented along the wafer miscut azimuth. The cross correlation was oriented along the growth direction and was not oblique, as reported earlier for a shorter period superlattice grown on a wafer with a ~10 times greater (4.3°) misorientation.[28] Atomic-force microscopy measurements were also performed on the sample. Mounds were seen on

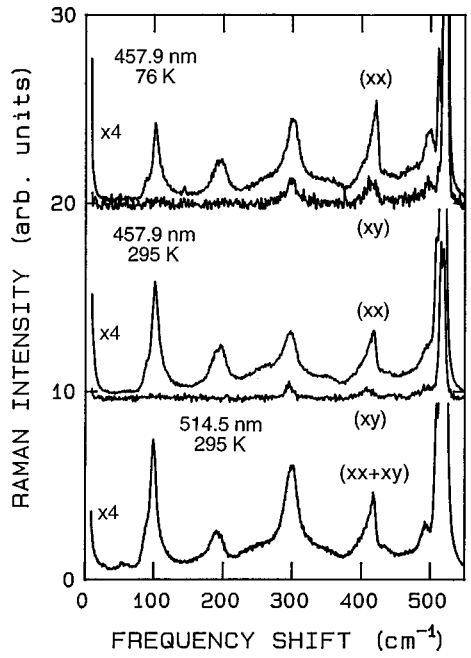

FIG. 1. Polarized $[z(xx)\bar{z};\ z(xy)\bar{z}]$ Raman spectrum of $(Si_{15}Ge_4)_{50}$ with excitation at 457.9 nm (at 76 K and 295 K) and the $z(xx+xy)\bar{z}$ spectrum with excitation at 514.5 nm (at 295 K).

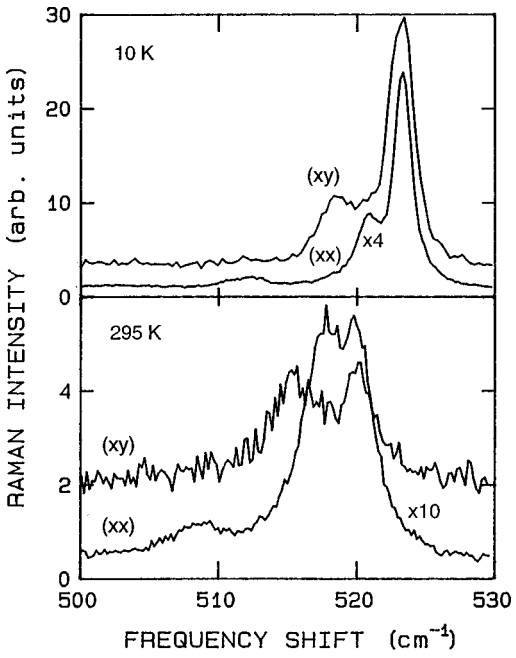

FIG. 2. Polarized $[z(xx)\bar{z};\ z(xy)\bar{z}]$ Raman spectrum of $(Si_{15}Ge_4)_{50}$ at 10 and 295 K in the region of the Si-layer confined modes. Excitation was at 457.9 nm.

the surface of size ~ 0.5 μm and amplitude 1 nm, approximately oriented along the miscut direction. The mounds do not form clear ripples, but are elongated along the direction of the surface steps.

Light-scattering measurements were carried out in a quasibackscattering geometry with the sample in a helium gas atmosphere to eliminate air features from the spectrum. Room-temperature measurements used an angle of incidence of 77.7° for the incoming laser light on the (001) surface. For low-temperature measurements the sample was mounted in the helium exchange gas of a Thor S500 cryostat with the angle of incidence increased to 85° to allow the specularly reflected component of the light beam to leave the cryostat cleanly. The temperature of the sample was monitored with a gold-iron/Chromel thermocouple mounted on the sample holder. Although there was inevitably some degree of laser heating it is estimated that the temperature of the sample could be maintained constant to within 2 K during a series of scans. The Raman spectrum was excited with 300 mW of 457.9-nm or 514.5-nm argon-laser light, analyzed with a Spex 14018 or SOPRA DMP2000 double monochromator, and detected with a cooled RCA 31034A or Hamamatsu R928P photomultiplier. The incident light was polarized in the scattering plane and the scattered light (collected at 90°) was either analyzed with Polaroid film or collected without polarization analysis. We describe the two polarization geometries used as being effectively $z(xx)\bar{z}$ or $z(xy)\bar{z}$ within the sample.[4]

III. RESULTS

The polarized Raman spectrum obtained with 457.9-nm excitation at a spectral resolution of 3 cm^{-1} is displayed in Fig. 1. In addition to the expected longitudinal optical (LO) phonon features around 300, 400, and 500 cm^{-1} there is prominent structure around 100 and 200 cm^{-1} in the $z(xx)\bar{z}$ spectrum which, as discussed in the next section, is assigned to folded longitudinal acoustic (FLA) modes of the superlattice with folding index $m=\pm 1$ and ± 2. These FLA features are notably strong in comparison with the LO scattering and the relatively small decrease in this strength on cooling the sample to a nominal 76 K confirms their first-order Raman character. The complete absence of the FLA features for the $z(xy)\bar{z}$ polarization geometry confirms their assignment and that there is minimal polarization breakthrough in the experiment. Thus, the weaker peaks seen in $z(xy)\bar{z}$ polarization in the optic-mode region (see Fig. 1) are allowed peaks.

It is seen that cooling the sample sharpens the LO features, particularly in the region of the Si-Si modes near 500 cm^{-1}. A scan of this region at a spectral resolution of 0.8 cm^{-1} (Fig. 2) clearly resolved peaks at room-temperature Raman shifts of 520, 518, and 509 cm^{-1} in $z(xx)\bar{z}$ polarization, and at 520 and 515.5 cm^{-1} in $z(xy)\bar{z}$ polarization. In Fig. 2, we also show the corresponding results for a nominal sample temperature of 10 K. Here the room-temperature structure is repeated, apart from a 3-cm^{-1} increase in peak wave-number shift and the appearance of further broad, weak structure in the region below 510 cm^{-1}. The strongest peak in both polarizations corresponds to the LO mode in bulk Si and is here identified with scattering from the superlattice substrate. The appearance of a substrate peak with this intensity indicates the Ge optical absorption in these thin layers is much less than that of bulk Ge at these wavelengths. The remaining peaks arise from Si-Si modes confined to the Si layers of the superlattice as discussed in the next section.

Of interest from the point of view of obtaining information about the relevant photoelastic constants is the intensity of the FLA peaks relative to the LA Brillouin peak ($m=0$). The relatively low background scattering from the surface of this sample enabled partial resolution of a Brillouin

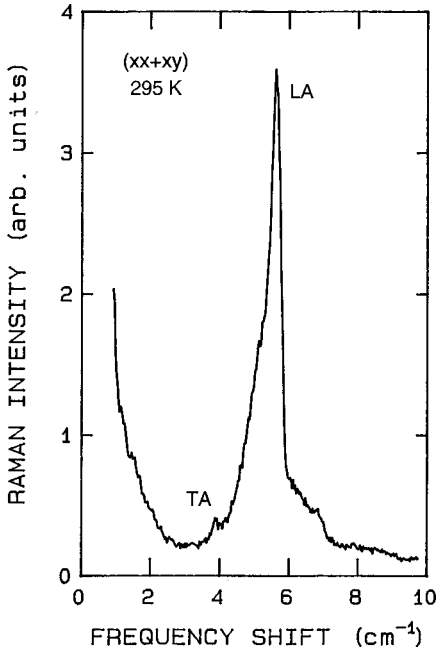

FIG. 3. Unpolarized $[z(xx+xy)\bar{z}]$ Brillouin spectrum of $(Si_{15}Ge_4)_{50}$ at 295 K with excitation at 457.9 nm.

peak at 5.4 cm^{-1} using the Spex monochromator at a spectral resolution of 0.6 cm^{-1}. On the SOPRA instrument, at a spectral resolution of 0.16 cm^{-1}, the structure of this Brillouin feature was clearly resolved, as displayed in Fig. 3. Comparison with the Brillouin spectrum of bulk Si under similar conditions revealed that the main peak, at 5.6 cm^{-1}, arises from the Si substrate LA mode and the weak feature at 3.8 cm^{-1} from the substrate transverse-acoustic (TA) mode. Again, the strength of these substrate features indicates a reduced Ge optical absorption. By a combination of subtraction of spectra and curve resolution the actual superlattice Brillouin peak was established to be at 5.2 cm^{-1} and its integrated intensity to be 54% of the total Brillouin scattering. A scan of the FLA ($m=\pm 1$) region under similar experimental conditions established the relative intensities for the photoelastic constant analysis.

IV. ANALYSIS

A. Acoustic modes

In the Rytov model,[29] which has become well established in this context for a range of superlattices,[1,2] the acoustic phonons are described by elastic waves propagating in a periodic structure with alternating layers characterized by a thickness d_i, a sound velocity v_i, and a density ρ_i ($i=1,2$) leading to an acoustic phonon-dispersion relation of the form

$$\cos(qd)=\cos\left(\frac{\omega d_1}{v_1}\right)\cos\left(\frac{\omega d_2}{v_2}\right) - \frac{1}{2}\left(K+\frac{1}{K}\right)\sin\left(\frac{\omega d_1}{v_1}\right)\sin\left(\frac{\omega d_2}{v_2}\right). \quad (1)$$

Here d is the superlattice period and $K=\rho_2 v_2/\rho_1 v_1$ is the ratio of the acoustic impedances of the two component layers. The effect of the superlattice periodicity is the folding back of the acoustic-phonon branch of the bulk crystal into a minizone, with maximum wave vector $q_{MZ}=\pi/d$. For phonon wave vector q away from such minizone boundaries the folded acoustic-phonon dispersion takes the linear form

$$\omega=V_{SL}|q+2\pi m/d|, \quad (2)$$

where $m=0,\pm 1,\pm 2,\ldots$ is the zone-folding index and V_{SL} is the appropriate superlattice acoustic velocity obtainable in Rytov's theory from the d_i, v_i, and ρ_i. For the quasiback-scattering geometry used here the relevant phonon wave vector is given by

$$q=\frac{4\pi n_{SL}(\lambda)}{\lambda}\left[1-\frac{1}{4[n_{SL}(\lambda)]^2}\right], \quad (3)$$

where $n_{SL}(\lambda)$ is the effective (mean) superlattice refractive index at the incident laser-light wavelength λ. In terms of the refractive indices of the component layers n_{SL} is given by

$$n_{SL}^2=(n_1^2 d_1+n_2^2 d_2)/d. \quad (4)$$

TABLE I. Mass density (ρ), sound velocity for longitudinal (ν^L) or transverse (ν^T) waves propagating in a [001] direction, and refractive indices (n) for bulk Si and Ge at 295 K, from Refs. 30 and 31.

	Si	Ge
ρ (kg/m^3)	2330	5323
ν^L (m/s)	8433	4914
ν^T (m/s)	5845	3542
n (457.9 nm)	4.66	3.98
n (514.5 nm)	4.27	4.51

The published values of the relevant parameters for bulk Si and Ge used in application of the Rytov theory here are listed in Table I. For the $(Si_{15}Ge_4)_{50}$ superlattice under consideration we find $q=0.101q_{MZ}$ for $\lambda=457.9$ nm and $q=0.085q_{MZ}$ for $\lambda=514.5$ nm. Solution of Eq. (1) for these phonon wave vectors gives the predicted Raman shifts listed in Table II, where they are compared with the observed features in the room-temperature Raman spectra. Here the Raman features in the 100- and 200-cm^{-1} regions have been curve-resolved to give the listed $m=\pm 1$ and $m=\pm 2$ peaks. The agreement with the Rytov model is excellent without any further adjustment of parameters. There is some evidence in the recorded spectrum (see Fig. 1) for $m=\pm 3$ and possibly $m=\pm 4$ FLA scattering around 260 and 350 cm^{-1}, respectively, but the situation is clouded by the overlap with the Ge-Ge LO mode and these features are at lower frequency than the Rytov model would predict.

As it is, the fit to the observed spectrum out to 200 cm^{-1} is a stringent test of the model, which is normally applied to Raman shifts of less than 100 cm^{-1}. We believe the Rytov model works so well here because the LA mode dispersion for both Si and Ge is close to linear well out into the normal first Brillouin zone.[30] Curvature of the LA mode dispersion will eventually lower the FLA mode frequencies below the Rytov model predictions and, furthermore, for $m=\pm 3$ and ± 4 modes, overlap with the optic-mode dispersion in the Ge layers would invalidate a simple elastic-wave treatment.

TABLE II. Experimental Raman peaks for $(Si_{15}Ge_4)_{50}$ at 295 K in the acoustic-phonon region and peak positions calculated using the Rytov model.

Mode assignment	Experimental ν (cm^{-1})		Calculated ν (cm^{-1})	
	$\lambda = 457.9$ nm	$\lambda = 514.5$ nm	$\lambda = 457.9$ nm	$\lambda = 514.5$ nm
LA ($m=0$)	5.2		4.8	4.1
FLA ($m=-1$)	88	89	89.8	90.3
FLA ($m=+1$)	102	100	102.7	102.2
FLA ($m=-2$)	188	189	187.1	187.8
FLA ($m=+2$)	198	198	197.4	196.7
FTA ($m=-1$)		54		62.9
FTA ($m=+1$)		62		72.0

Included in Table II are two additional weak peaks seen with 514.5-nm excitation (Fig. 1). Although similar features were not seen with 457.9-nm excitation, they are possibly associated with folded transverse-acoustic (FTA) modes, weakly allowed as a result of the small departure from an exact backscattering geometry. A Rytov-model calculation using the appropriate TA wave velocities (Table I) is seen to predict higher Raman shifts than the observed features. Reduction of the ν^T values by 10%, however, gives a much closer match to experiment and such a reduction is not unreasonable in view of the known TA phonon dispersion for Si and Ge.[30]

Before closing this section on acoustic phonons we remark briefly on additional structure in the region of the Brillouin peak (see Fig. 3). Clearly there is some extra scattering on the high-energy side of the substrate Brillouin peak in the region of 6.5 and 8.5 cm^{-1}. Similar features have been reported previously[32] in ultrathin Ge_mSi_n superlattices and were there identified with resonant-phonon modes arising from the interaction between the continuum of acoustic modes of the Si substrate and the quasilocalized superlattice modes. The extra scattering observed here is likely to be of similar origin, although the expected mode interval of about 1 cm^{-1} for an overall superlattice thickness of 129 nm (50×2.58 nm) is not resolved.

B. Photoelastic constants

We now consider what information can be extracted from the observed relative intensities of the FLA scattering. The experimental intensity data for 457.9 nm excitation are summarized in Table III. Since cooling the sample did not result in any significant narrowing of the FLA features we have restricted our attention to the room-temperature spectrum. The inability to resolve the $\pm m$ components experimentally places a significant restriction on our knowledge of the intensities of these individual components relative to the superlattice Brillouin intensity (I_0). Attempts to resolve the $m = \pm 1$ and $m = \pm 2$ features by curve fitting led to a range of possibilities, which is reflected in the relatively high uncertainties for I_{+1}/I_{-1} and I_{+2}/I_{-2}. The problem here is knowing what allowance to make for the broad underlying background scattering, which is clearly present in the recorded spectrum. The varying background (possibly second-order Raman) is obviously a problem for the $m = \pm 2$ peak, but also affects the $m = \pm 1$ peak, where the asymmetric line shape indicates some extra scattering on the high-frequency side.

The first attempt to model the intensities of superlattice FLA features was that of Colvard *et al.*[20] who proposed a photoelastic mechanism for the light scattering. In their treatment, which assumed the same sound velocity in each layer, the intensities of the $+m$ and $-m$ components are equal for a given m and the ratio of that intensity I_m to that of the Brillouin scattering ($m=0$) is given by

$$\frac{I_m}{I_0} = \frac{(P_b - P_a)^2}{P_0^2} \frac{\sin^2(m\pi d_1/d)}{\pi^2 m^2} \frac{\omega_m(n_m+1)}{\omega_0(n_0+1)}. \quad (5)$$

Here P_a and P_b are the photoelastic constants for the two types of layer and are assumed to be real quantities, n_m and n_0 are the relevant Bose-Einstein population factors at the sample temperature, and P_0 is given by

$$P_0 = \frac{1}{d}(d_1 P_a + d_2 P_b). \quad (6)$$

For the sample studied here, the observed $I_{\pm 1}$ (average) ($=\overline{I}_{\pm 1}$) to I_0 ratio of 1.36 ($\pm 15\%$) gives two possible solutions of Eqs. (5) and (6) for the ratio of the photoelastic constants of Ge and Si: $P_{Ge} = -1.8(\pm 0.1)P_{Si}$ or $P_{Ge} = -56(+23,-180)P_{Si}$. The observed ratio $\overline{I}_{\pm 2}/\overline{I}_{\pm 1}$ differs, however, from the prediction of Eq. (5) by a factor of 2 and it is clear that I_{-1} and I_{+1} are not equal so that the model of Colvard *et al.* cannot be considered valid here.

A more detailed analysis of the propagation of LA phonons along the axis of a superlattice has been presented by He, Djafari-Rouhani, and Sapriel,[24] who included the effects of acoustic and also dielectric mismatch between the layers. In an attempt to improve on the predictions of Colvard *et al.* for our sample we have applied Eq. (58) of Ref.

TABLE III. Relative intensities of FLA features from the Raman spectrum of $(Si_{15}Ge_4)_{50}$ at 295 K excited with 457.9-nm radiation. The $\overline{I}_{\pm 1}/I_0$ ratio was obtained using the SOPRA spectrometer.

$\frac{\overline{I}_{\pm 1}}{I_0}$	$\frac{I_{+1}}{I_{-1}}$	$\frac{I_{-1}}{I_0}$	$\frac{I_{+1}}{I_0}$	$\frac{I_{+2}}{I_{-2}}$	$\frac{\overline{I}_{\pm 2}}{I_{\pm 1}}$
1.36 ± 0.20	13 ± 5	0.19 ± 0.07	2.5 ± 1.0	0.91 ± 0.22	0.42 ± 0.05

24 to evaluate the expected FLA intensity ratios for a range of P_{Ge}/P_{Si} values. [It is noted that there is an m-dependent factor of ω_m^{-2} (or ω_p^{-2} in the notation of He *et al.*) missing from Eq. (58) of Ref. 24.] Although the effect is small at room temperature, we have included the $\omega_m(n_m+1)$ factor of Eq. (5) above to take account of the finite temperature of our sample. The results of this analysis, which treats the superlattice as a homogeneous medium as regards to the propagation of incident or scattered light [i.e., neglects any difference in refractive index between the layers, using the mean refractive index n_{SL} of Eq. (4)], are presented in Fig. 4(a). It is seen that the relative intensities I_{+1}/I_{-1} and I_{+2}/I_{-2} differ significantly from 5 and 0.46, respectively, only in a restricted range either side of $P_{Ge}/P_{Si}=1$. In this region I_{-1}/I_0 and I_{+1}/I_0 both fall to zero and vary rapidly for $-3<P_{Ge}/P_{Si}<0$. A similar pattern occurs for $m=\pm 2$. It is of interest to note that the ratio $\overline{I}_{\pm 2}/\overline{I}_{\pm 1}$ is predicted to be 0.54 throughout most of the range $-55<P_{Ge}/P_{Si}<+55$, dropping slightly below this for $0.6<P_{Ge}/P_{Si}<1.4$. The $m=\pm 2$ mode intensities are expected to be more sensitive to the quality of the superlattice, and to any acoustic attenuation and optical absorption effects[33] than the $m=\pm 1$ components. Comparison of the experimental $\overline{I}_{\pm 2}/\overline{I}_{\pm 1}$ ratio of 0.42 with the predicted 0.54 confirms the high quality of our sample and suggests that absorption effects are not dominant. Nevertheless, we take the I_m/I_0 ratios for $m=\pm 1$ to be the more reliable measure of the photoelastic properties. The I_{+m}/I_{-m} ratios should not be particularly sensitive to superlattice quality or absorption effects, but, because the individual contributions are not clearly resolved, these ratios have large experimental uncertainties.

Detailed inspection of Fig. 4(a) reveals no P_{Ge}/P_{Si} value for which the four plotted ratios fit the experimental ratios (Table III) within the estimated uncertainties. In particular, one cannot simultaneously fit I_{-1}/I_0 and I_{+1}/I_0 because, for the $P_{Ge}/P_{Si}\cong 0.6$ needed to fit the observed I_{+1}/I_{-1} ratio, the predicted I_{-1}/I_0 and I_{+1}/I_0 ratios are an order of magnitude or more too small. In view of the difficulty of resolving I_{-1} from I_{+1}, we consider $\overline{I}_{\pm 1}/I_0$ to give $P_{Ge}=-1.21(\pm 0.07)P_{Si}$ as a compromise ''best fit'' in this model.

To what extent is the failure to obtain a good fit to the experimental intensity ratios a result of neglecting the difference in refractive index between the layers? Although the example considered by He *et al.* suggested that the effect of varying the refractive index should not be significant for q within the first Brillouin zone, which is the case we consider here, the possibility cannot be discounted that the effect might be significant for the layer thicknesses in our sample. To investigate the effect of the refractive index inhomogeneity of the Si/Ge superlattice the relevant intensities have been recalculated using an algorithm based on a Green's-function formalism[34] and the results are presented in Fig. 4(b). On comparison with Fig. 4(a) it is seen that the refractive-index variation has essentially no effect on the predicted I_{+2}/I_{-2} ratio, but that the other plotted ratios are all reduced a little compared to the ''mean refractive-index'' model. A similar pattern of dependence on P_{Ge}/P_{Si} pertains, however, and again it is not possible to fit the four plotted intensity ratios.

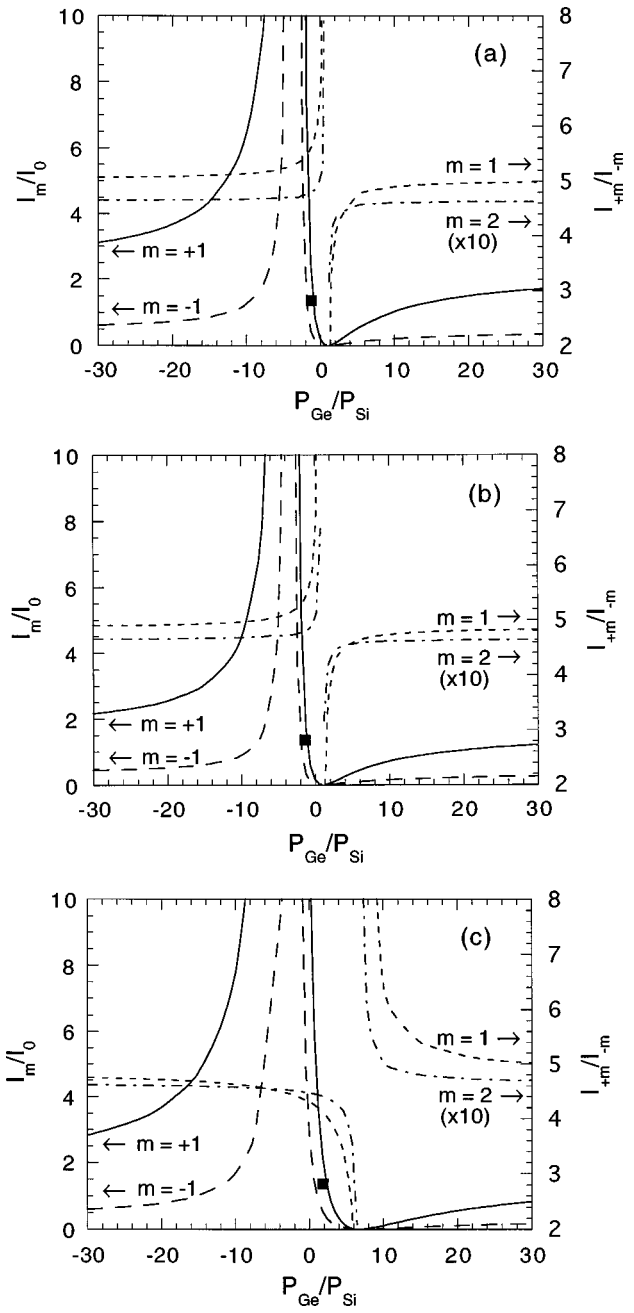

FIG. 4. Predicted relative Raman-scattering intensities, I_m/I_0 (left scale) and I_{+m}/I_{-m} (right scale), of FLA modes ($m=1,2$) of $(Si_{15}Ge_4)_{50}$ as a function of the P_{Ge}/P_{Si} photoelastic-coefficient ratio. (a) Based on Eq. (58) of He, Djafari-Rouhani, and Sapriel (Ref. 24). (b) Including the effect of dielectric mismatch between the layers, but not interface translational displacement (Ref. 34). (c) Including the effects of dielectric mismatch and interface translational displacement (Ref. 34). In each case the relative intensities plotted refer to folding index (m) values of $-1/0$ (long dashes), $+1/0$ (solid line), $+1/-1$ (short dashes), and $+2/-2$ (dash-dot).

For this model the observed $\overline{I}_{\pm 1}/I_0$ ratio would give $P_{Ge}=-1.40(\pm 0.08)P_{Si}$ as the compromise fit, although now, if one completely ignores the observed I_{+m}/I_{-m} ratios, P_{Ge}/P_{Si} values in the range -30 to -45 would also match the observed $\overline{I}_{\pm 1}/I_0$.

In their development of the formalism we have used here to treat the refractive-index variation, Djafari-Rouhani and

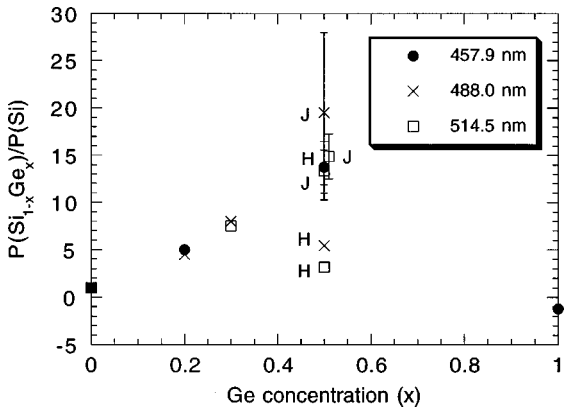

FIG. 5. Comparison of the photoelastic-coefficient ratio $P(\mathrm{Si}_{1-x}\mathrm{Ge}_x)/P(\mathrm{Si})$ for various values of x from earlier studies with the $x=1$ value obtained here. As discussed in the text, H and J label recalculated results from the measurements of He, Sapriel, and Brugger (Ref. 21) and Jin *et al.* (Ref. 22), respectively.

Khourdifi[34] identified a further contribution to the FLA-scattered intensities that results from the translational displacement of interfaces during a longitudinal vibration in the presence of a mismatch between the dielectric constants of the superlattice constituents. Djafari-Rouhani and Khourdifi identify this effect as the analogue of the surface-wave (ripple) contribution[35] to the usual elasto-optic Brillouin scattering from bulk materials. Since the contribution from this extra term was available to us[34] and no comparison with experiment has been made before, we present the results of including it in Fig. 4(c). Here we see some significant changes cf. Figs. 4(a) and 4(b). In particular, the region of divergence of the I_{+m}/I_{-m} ratios from their limiting values is displaced to the vicinity of $P_{\mathrm{Ge}}=+7P_{\mathrm{Si}}$ and their variation as $P_{\mathrm{Ge}}/P_{\mathrm{Si}}$ approaches this region is reversed compared to the previous results. Clearly this interface translational-displacement effect is significant for our sample, but we are no closer to a satisfactory fit of the observed intensity ratios. We are left with yet another compromise fit of $\overline{I}_{\pm 1}/I_0$ at $P_{\mathrm{Ge}}=+1.8(\pm 0.2)P_{\mathrm{Si}}$.

Overall, our failure to obtain a satisfactory fit of the observed FLA relative intensities suggests that there must be other contributions not yet considered. From our analysis it would seem that P_{Ge} and P_{Si} are most probably of a similar magnitude, although they could possibly have opposite signs. It is worth noting that our earlier conclusion concerning superlattice quality and absorption effects is reinforced by consideration of the refractive-index variation. Either with or without inclusion of the interface-vibration contribution the predicted value of $\overline{I}_{\pm 2}/\overline{I}_{\pm 1}$ falls in the range 0.490–0.495 for almost the entire range of $P_{\mathrm{Ge}}/P_{\mathrm{Si}}$ values considered. This prediction is even closer to the observed value of 0.42 than that from the mean n_{SL} model.

In Fig. 5 we make a comparison of earlier measures of photoelastic constant ratios for $\mathrm{Si}/\mathrm{Si}_{1-x}\mathrm{Ge}_x$ superlattices[21–23] with our result for Si/Ge. A word of caution is needed here as the photoelastic constants used by He, Sapriel, and Brugger[21] in their follow-up study of $\mathrm{Si}/\mathrm{Si}_{0.5}\mathrm{Ge}_{0.5}$ differ from those used in the other earlier paper by a factor of $(-n^4)$, where n is the refractive index at the laser wavelength used. Furthermore, we note that the refractive indices used by He, Sapriel, and Brugger[21] are a linear interpolation between the Si and Ge values at each wavelength considered. A subsequent study of $\mathrm{Si}_{1-x}\mathrm{Ge}_x$ alloys[31] has revealed that the actual $\mathrm{Si}_{0.5}\mathrm{Ge}_{0.5}$ refractive indices differ significantly from the values used by He, Sapriel, and Brugger. In order to make a valid comparison we have, therefore, reevaluated the He, Sapriel, and Brugger intensity-ratio data on the basis of the mean n_{SL} model [using $n(514.5\ \mathrm{nm})=5.04$, $n(488.0\ \mathrm{nm})=5.34$, and $n(457.9\ \mathrm{nm})=5.64$ for the $\mathrm{Si}_{0.5}\mathrm{Ge}_{0.5}$ alloy] to give the points labeled H in Fig. 5. While the $\lambda=514.5$ nm fit is unambiguous, there is an increasing discrepancy between the photoelastic ratio giving a fit to the observed I_{-1}/I_0 and that giving a fit to I_{+1}/I_0 as one goes to shorter laser wavelengths, i.e. as was the case with our sample, one cannot fit these two ratios and the observed I_{+1}/I_{-1} simultaneously. For $\lambda=457.9$ nm a range of 11.9 to 15.6 for $P_{\mathrm{alloy}}/P_{\mathrm{Si}}$ is needed to cover the measured intensities. For consistency we have also reevaluated the $\mathrm{Si}/\mathrm{Si}_{1-x}\mathrm{Ge}_x$ results of Jin *et al.*,[22] using the same mean n_{SL} model, to give the $x=0.5$ points and the $x=0.51$ point labeled J in Fig. 5. Again we have been unable to obtain a consistent fit (in these cases even for 514.5-nm laser excitation) and the uncertainty bars in Fig. 5 indicate the range of photoelastic constant ratios needed. Within these uncertainties our results encompass the values reported in Ref. 22 (in which essentially the same mean n_{SL} model was used[36]), but analysis of the $\lambda=514.5$ nm spectrum for $x=0.51$ was not reported by Jin *et al.* Clearly the discrepancy between the $x=0.5$ results in Refs. 21 and 22 is not resolved by correcting the refractive indices used in the analysis.

Overall the data presented in Fig. 5 indicate a strong x dependence for the $P_{\mathrm{alloy}}/P_{\mathrm{Si}}$ ratio. In the $x\rightarrow 0$ limit this ratio of photoelastic constants must approach 1. While it would appear to increase significantly as x is increased to 0.5, our results here suggest that this ratio must subsequently decrease again as $x\rightarrow 1$. Such a wide variation with alloy composition should not, perhaps, be unexpected in view of the variation of refractive index[31] with x, since both effects depend in some way on the electronic structure of the alloy and the way it interacts with light. Much further work is needed, however, to give a clear picture of the x dependence of the photoelastic constant ratio for the $\mathrm{Si}_{1-x}\mathrm{Ge}_x/\mathrm{Si}$ system. Our analysis has indicated that there are still significant hurdles, both theoretical and experimental, to be overcome before a satisfactory understanding is reached. Certainly it would appear that the interface translational displacement contribution to FLA intensities cannot be dismissed.

C. Optic modes

In the usual slab-mode model, first applied to GaAs/AlAs superlattices,[37,38] the confined optical phonons in the Si layers of the superlattice can be assigned an effective wave vector k_m:

$$k_m=\pi m/(n+\delta)d_0, \quad m=1,2,\ldots,n. \tag{7}$$

Here n is the layer thickness in monolayers (each of thickness d_0) and m is the mode index (giving $m+1$ displacement

nodes along the normal of each Si layer). δ represents the spread of the mode into the surrounding second material. Following earlier calculated[17] and experimental[13] results for Si/Ge superlattices we take $\delta=1$, although the precise choice of δ within the usual range 0–1 is not significant in comparison with our experimental uncertainties.

The observed room-temperature Raman peaks at 518, 515.5, and 509 cm^{-1}, corresponding to $m=1$, 2, and 3, respectively, give a close match to the LO phonon dispersion along [001] of bulk Si,[30] as was the case in an earlier study of short period (001) Si/Ge superlattices.[13] The new feature here is the observation that the $m=1$ and 3 slab modes appear in $z(xx)\bar{z}$ polarization, while the $m=2$ mode (not previously seen for Si) appears in $z(xy)\bar{z}$ polarization. Such an even/odd index polarization pattern has been previously reported for the corresponding confined modes in GaAs/AlAs superlattices, but in that case the even [odd] index modes appeared in $z(xx)\bar{z}$ [$z(xy)\bar{z}$] polarization.[37,38] Our Si/Ge superlattice, grown along the [001] direction, comprises 19 monolayers per period. According to the symmetry analysis of Alonso, Cardona, and Kanellis[39] the appropriate space-group symmetry is $I4_1/amd$. Here the odd index Si-Si modes have A_{1g} symmetry and the even modes are of B_{1g} symmetry, which is consistent with the observed diagonal and off-diagonal polarizations.

The Ge-Ge and Si-Ge LO mode peak wave numbers for 457.9- (514.5-) nm excitation are 297 (300) and 417 (418) cm^{-1}, respectively, at 295 K. These correspond to frequencies generally matching theoretical predictions for the two modes.[14–17] The observed dispersion with wave-vector change from $q(514.5\ \mathrm{nm})=0.085q_{\mathrm{MZ}}$ to $q(457.9\ \mathrm{nm})=0.101q_{\mathrm{MZ}}$ of the quasiconfined Ge-Ge mode is in accord with the dispersion of bulk Ge.[30] The small shift in the Si-Ge LO mode is consistent with model calculations[15] indicating some degree of alloying across the layer interface.

In $z(xy)\bar{z}$ polarization with 457.9-nm excitation, weak bands occur at 295 and 408 cm^{-1}. These features in the spectrum are analogues of the Ge-Ge and Si-Ge modes discussed above, but are shifted to lower frequency by 2–9 cm^{-1}. The polarization of these modes suggests they are quasi-transverse-optical (TO) vibrations. This is confirmed by their frequencies, which reflect the similar LO-TO splittings observed at small wave vectors in bulk Ge and Si.[30] Calculations for Si_6Ge_6 superlattices reveal a similar LO-TO relationship.[17] The broader and more symmetric line shape observed here for the Si-Ge TO mode compared to the LO mode reproduces the observations of de Gironcoli *et al.*[15] in their Raman microprobe study of this interface mode using an in-plane scattering geometry.

V. CONCLUSIONS

Raman spectra obtained from a high-quality $(Si_{15}Ge_4)_{50}$ atomic-layer superlattice have allowed for the first time a detailed analysis of the photoelastic coefficient ratio $P_{\mathrm{Ge}}/P_{\mathrm{Si}}$ from FLA mode intensities. An extensive comparison with existing theoretical models shows $|P_{\mathrm{Ge}}/P_{\mathrm{Si}}|\cong 1$ at 457.9 nm. However, a satisfactory fit to all the experimental data could not be obtained, and the same problem was found to exist with two earlier studies of FLA modes in $Si/Si_{0.5}Ge_{0.5}$ superlattices. The present analysis indicates a need for revisions to current models of FLA mode Raman intensities. The existing difficulties may be alleviated by consideration of complex photoelastic coefficients in the theory for opaque semiconductors, as in the present case of Si and Ge at visible wavelengths. Whatever revisions are made, this paper has clearly shown the need for careful consideration of the interface translational-displacement contribution to the inelastic light-scattering cross section. The photoelastic-coefficient ratio obtained here may differ appreciably from that found in bulk material owing to electronic-confinement effects in this thin-layer superlattice modifying the optical response, especially for the Ge layers.

The odd and even index confined optic modes observed for the Si layers of the superlattice are readily interpreted in the slab-mode model that has found equal success in III-V systems. Two lower-frequency quasiconfined optic modes exhibit dispersion that is consistent with previous model calculations.

ACKNOWLEDGMENTS

We thank H. J. Labbé and E. Estwick for technical assistance, B. Djafari Rouhani for comments on the photoelastic coefficient calculations, and Jin Ying for further details of his work.[8,22]

*Permanent address: Department of Physics and Astronomy, University of Canterbury, Private Bag 4800, Christchurch, New Zealand.

[1] B. Jusserand and M. Cardona, in *Light Scattering in Solids V*, edited by M. Cardona and G. Güntherodt (Springer, Heidelberg, 1989), p. 49.

[2] J. Sapriel and B. Djafari Rouhani, Surf. Sci. Rep. **10**, 189 (1989).

[3] H. Brugger, G. Abstreiter, H. Jorke, H. J. Herzog, and E. Kasper, Phys. Rev. B **33**, 5928 (1986).

[4] D. J. Lockwood, M. W. C. Dharma-wardana, J.-M. Baribeau, and D. C. Houghton, Phys. Rev. B **35**, 2243 (1987).

[5] E. Kasper, H. Kibbel, H. Jorke, H. Brugger, E. Friess, and G. Abstreiter, Phys. Rev. B **38**, 3599 (1988).

[6] H. Brugger, E. Friess, G. Abstreiter, E. Kasper, and H. Kibbel, Semicond. Sci. Technol. **3**, 1166 (1988).

[7] M. I. Alonso, F. Cerdeira, D. Niles, M. Cardona, E. Kasper, and H. Kibbel, J. Appl. Phys. **66**, 5645 (1989).

[8] Y. Jin, S. L. Zhang, G. G. Qin, G. L. Zhou, and M. R. Yu, J. Phys.: Condens. Matter **4**, 3867 (1992).

[9] P. X. Zhang, D. J. Lockwood, H. J. Labbé, and J.-M. Baribeau, Phys. Rev. B **46**, 9881 (1992).

[10] M. W. C. Dharma-wardana, P. X. Zhang, and D. J. Lockwood, Phys. Rev. B **48**, 11 960 (1993).

[11] J. Menéndez, A. Pinczuk, J. Bevk, and J. P. Mannaerts, J. Vac. Sci. Technol. B **6**, 1306 (1988).

[12] E. Friess, H. Brugger, K. Eberl, G. Krötz, and G. Abstreiter, Solid State Commun. **69**, 899 (1989).

[13] E. Friess, K. Eberl, U. Menczigar, and G. Abstreiter, Solid State Commun. **73**, 203 (1990).

[14] M. W. C. Dharma-wardana, G. C. Aers, D. J. Lockwood, and J.-M. Baribeau, Phys. Rev. B **41**, 5319 (1990).

[15] S. de Gironcoli, E. Molinari, R. Schorer, and G. Abstreiter, Phys.

Rev. B **48**, 8959 (1993); R. Schorer, G. Abstreiter, S. de Gironcoli, E. Molinari, H. Kibbel, and H. Presting, *ibid.* **49**, 5406 (1994).

[16] A. Fasolino, E. Molinari, and J. C. Maan, Phys. Rev. B **39**, 3923 (1989).

[17] E. Molinari and A. Fasolino, Appl. Phys. Lett. **54**, 1220 (1989).

[18] A. Qteish and E. Molinari, Phys. Rev. B **42**, 7090 (1990).

[19] J. Zi, K. Zhang, and X. Xie, J. Phys.: Condens. Matter **3**, 6239 (1991).

[20] C. Colvard, T. A. Gant, M. V. Klein, R. Merlin, R. Fischer, and H. Morkoç, Phys. Rev. B **31**, 2080 (1985).

[21] J. He, J. Sapriel, and H. Brugger, Phys. Rev. B **39**, 5919 (1989).

[22] Y. Jin, S. L. Zhang, Y. L. Fan, M. R. Yu, X. Wang, and G. G. Qin, Superlattices Microstruct. **12**, 73 (1992).

[23] T. A. Gant, D. J. Lockwood, J.-M. Baribeau, and A. H. MacDonald, in *Spectroscopy of Semiconductor Microstructures*, edited by G. Fasol, A. Fasolino, and P. Lugli (Plenum, New York, 1989), p. 235.

[24] J. He, B. Djafari-Rouhani, and J. Sapriel, Phys. Rev. B **37**, 4086 (1988).

[25] J.-M. Baribeau, T. E. Jackman, D. C. Houghton, P. Maigné, and M. W. Denhoff, J. Appl. Phys. **63**, 5738 (1988).

[26] J.-M. Baribeau, D. J. Lockwood, M. W. C. Dharma-wardana, N. L. Rowell, and J. P. McCaffrey, Thin Solid Films **183**, 17 (1989).

[27] J.-M. Baribeau, D. J. Lockwood, and R. W. G. Syme, J. Appl. Phys. **80**, 1450 (1996).

[28] R. L. Headrick, J.-M. Baribeau, and Y. E. Strausser, Appl. Phys. Lett. **66**, 96 (1995).

[29] S. M. Rytov, Akust. Zh. **2**, 71 (1956) [Sov. Phys. Acoust. **2**, 68 (1956)].

[30] *Numerical Data and Functional Relationships in Science and Technology*, edited by O. Madelung, Landolt-Börnstein, New Series, Group III, Vol. 17, Pt. a (Springer-Verlag, Berlin, 1982), pp. 63, 76, 105, 119, 370, and 411, and references therein.

[31] J. Humlíček, M. Garriga, M. I. Alonso, and M. Cardona, J. Appl. Phys. **65**, 2827 (1989).

[32] D. J. Lockwood, M. W. C. Dharma-wardana, G. C. Aers, and J.-M. Baribeau, Appl. Phys. Lett. **52**, 2040 (1988).

[33] J. He, J. Sapriel, and R. Azoulay, Phys. Rev. B **40**, 1121 (1989).

[34] B. Djafari-Rouhani and E. M. Khourdifi, in *Light Scattering in Semiconductor Structures and Superlattices*, edited by D. J. Lockwood and J. F. Young (Plenum, New York, 1991), p. 139. We thank B. Djafari-Rouhani for making available to us a computer algorithm incorporating the results of this work.

[35] J. R. Sandercock, in *Light Scattering in Solids III*, edited by M. Cardona and G. Güntherodt (Springer-Verlag, Berlin, 1982), p. 173.

[36] Y. Jin (private communication).

[37] A. K. Sood, J. Menéndez, M. Cardona, and K. Ploog, Phys. Rev. Lett. **54**, 2111 (1985).

[38] D. J. Mowbray, M. Cardona, and K. Ploog, Phys. Rev. B **43**, 1598 (1991).

[39] M. I. Alonso, M. Cardona, and G. Kanellis, Solid State Commun. **69**, 479 (1989).